Oil Shale, 2016, Vol. 33, No. 3, pp. 216–227
doi: 10.3176/oil.2016.3.02

ISSN 0208-189X

APPROACHES TO IMPROVING THE POROSITY AND PERMEABILITY OF MAOMING OIL SHALE, SOUTH CHINA

YUANPING GAO*, QIULIAN LONG, JIANZHENG SU, JIAYUAN HE, PENG GUO

Petroleum Exploration and Production Research Institute of SINOPEC, Beijing 100083, China

Abstract. *This work aims at developing suitable means to improve the porosity and permeability of oil shale formations. The pulse power fracturing technology (PPFT) is designed and applied to the Maoming oil shale block in South China and its effect is assessed by conducting ultrasonic wave and hydraulic pressure drop tests. The test results show that stimulation can be effectively applied to the oil shale formation. The treatment agent post-processing technology (TAPT) is designed and tested using oil shale samples from the Maoming block. The experimental results demonstrate that the porosity, pyrolysis rate and oil yield of oil shale samples can be increased by more than 25% after applying the treatment agent. The study concludes that PPFT and TAPT have great potential to be effectively used for the stimulation of oil shale formations.*

Keywords*: oil shale in-situ exploitation, stimulation, permeability, pulse power fracturing technology, treatment agent.*

1. Introduction

Oil shale is an organic-rich sedimentary rock containing a significant amount of organic matter called kerogen. It is highly abundant worldwide and is regarded as a potential energy resource alternative to oil and gas [1]. Recent statistics suggest that the total world oil shale resources are equivalent to 411 billion tons of oil [2]. China has the second largest oil shale resource in the world, containing approximately 47.6 billion tons of oil. The oil shale deposits in China have three typical features. First, the mines are relatively shallow, with 64% of oil shale buried at a depth less than 500 m. Second, most of the oil shale layers are rather thin, with an average thickness of 20–30 m. Third, high-quality oil shale with an oil yield over 10% accounts

---

[*] Corresponding author: e-mail *gaoyp.syky@sinopec.com*

for only 17.6%, while the oil yield of oil shale in almost half of the mines is less than 5% [3, 4]. The Maoming block in South China has similar features as noted above and is used as the target in this study. Uncovering the formation conditions and developing suitable stimulation methods are of high significance for an effective exploitation of oil shale resources.

Oil shale is generally exploited in two ways: surface retorting or in-situ retorting. Surface retorting has been commercially applied in many countries since it has advantages of quick economic returns and relatively low technological requirements. However, this method may cause serious environmental pollution problems, extensive waste of water and is feasible to be used only in shallow oil shale mines. In-situ retorting obviates the problems of handling large quantities of material, as well as offers the potential for recovering deeply deposited oil shale resources. Under the increasing pressure on environmental protection, the in-situ process has become an inevitable trend of the large-scale commercial exploitation of oil shale resources [5, 6].

During the past decades, researchers, mainly from international oil companies, have been doing remarkable work on the in-situ exploitation of oil shale, and have reported several inspiring inventions, such as Shell's In-situ Conversion Process (ICP) technology [7, 8], ExxonMobil's Electrofrac technology [9], Chevron's CRUSH technology [10] and the U.S. Shale Oil company's Conduction, Convection and Reflux (CCR) technology [11]. These technologies employ different heating methods such as electric heating, thermal fluid heating, radiant heating and combustion heating. Among them, the ICP technology is relatively well developed and has been tested by Shell Company in the Green River Formation in western USA. However, long heating period, about 2–4 years, is needed because of slow heating rate, resulting in high power consumption and poor economic performance especially for thin layers. In September 2013, Shell announced its withdrawal from Research, Development & Demonstration (RD&D) projects on Green River oil shale.

Thermal fluid heating technology has been arousing more and more interest because of its fast heating speed and capability to take full advantage of carbonization gas. However, usually thermal fluid cannot be directly injected into the formation due to the extremely low permeability of oil shale. In order to improve the permeability, reservoir stimulation is necessary. Maoming oil shale resources have three common features. First, the main components of oil shale are clay minerals. The total content of kaolinite, hydromica and montmorillonite ranges from 50 to 70%. At the same time, the total content of brittle minerals varies from 30 to 40% [12], which is lower than the 60% required for forming a network of fractures by hydraulic fracturing. Second, the main seam is very shallow, mostly at a depth less than 300 m. Thus the horizontal stress is usually higher than the vertical stress. Lastly, horizontal beddings are well developed. As a result, the effect of stimulation using hydraulic fracturing is usually unsatisfactory because only horizontal fractures can be formed easily. Developments of other effective means for increasing the permeability of oil shale are needed.

In this study, the pulse power fracturing technology (PPFT) is designed and applied to the Maoming oil shale block in South China, and its effect is assessed. The treatment agent post-processing technology (TAPT) is designed and tested using oil shale samples from the Maoming block. The results will be presented and interpreted in the following sections.

2. Theory and experiments

2.1. Samples and properties

In this study, oil shale samples from the Maoming block were used. The results of Fischer assay and proximate analysis of Maoming oil shale are given in Tables 1 and 2, respectively.

Table 1. Fischer assay of Maoming oil shale

Oil, ar, %	Moisture, ar, %	Semicoke, ar, %	Gas and loss, ar, %
9.36	6.80	78.59	5.25

Note: ar – as received.

Table 2. Proximate analysis of Maoming oil shale

M_{ar}, %	V_{ar}, %	A_{ar}, %	FC_{ar}, %	$Q_{net,ar}$, kJ/kg
2.85	70.65	21.35	5.15	8.81

Note: $_{ar}$ – as received.

2.2. Pulse power fracturing technology

High power pulse is a tool to generate strong electric pulses. The energy is stored in a slow way (in the order of magnitude of seconds). The pulse compression and power amplification are achieved by various fast-changing switches. High power electromagnetic energy is instantaneously released to the load in a very short time (in the order of magnitude of microseconds to nanoseconds) with high power (MW to GW) in the form of a single pulse or controlled repetitive pulses. Repetitively pulsed shock waves are generated by a high power electric device. When the reservoir is impacted by the shock wave, it acts as both the action object and the propagation medium for the shock wave. If the peak pressure of the shock wave is higher than the breaking limit, the reservoir formation will be fractured. In this study, the fracturing technique designed on the basis of high power pulse technology is named pulse power fracturing technology (PPFT).

Repetitively pulsed strong shock waves generated using the electrohydraulic effect can be explained by two mechanisms. One is that the plasma channel discharged in water rapidly expands and generates a strong shock wave with the heating of the discharge current. The other consists in that the plasma channel discharged in water heats the water molecules around, causing a rapid heating-up, vaporization and expansion, and then the formation of a strong shock wave. The peak pressure of these shock waves can be calculated by Equations 1 [13] and 2 [14], respectively:

$$P = \beta\sqrt{\frac{\rho w}{\tau T}}\,, \tag{1}$$

$$P = k\frac{C^{1/2}U}{1.4r^{5/2}}\,, \tag{2}$$

where P is the peak pressure of the shock wave, Pa; β is a complex integration, the value of which is 0.7 in water, dimensionless; ρ is the water density, kg/m^3; τ is the leading edge of the shock wave, s; T is the bottom width of the shock wave, s; w is the total energy of the discharge current per unit length of the discharge channel, J/m; k is the coefficient, dimensionless; C is the electric capacity, F; U is the voltage, kV; r is the spreading distance of the shock wave, m.

It is shown by Equations 1 and 2 that the peak pressure of the shock wave is proportional to the discharge energy and the energy density of the discharge channels. It is also proportional to the storage capacity and the square of the discharge voltage in a condition of constant storage energy. The electrical energy density in the energy storage component is a major obstacle to the application of the shock wave. In order to apply the repetitively pulsed shock wave to unconventional gas development and to generate stronger shock waves in the limited space, a comprehensive study of energy conversion efficiency as well as uncovering the related physical mechanisms are necessary.

2.3. Treatment agent post-processing technology

By employing PPFT, one can break the oil shale formation and create fractures, which is useful for the injection of a thermal fluid into it. If the treatment agent is injected into the formation after using PPFT, it will promote the development of fractures therein and increase permeability. As a result, it eases the injection of the thermal fluid and renders the in-situ exploitation using heating with fluid more efficient. In the current study, this technology is named the treatment agent post-processing technology (TAPT).

The mass fractions of components in the developed treatment agent are as follows: acid 5–28%, cobalt and/or nickel salt 0.1–1%, inhibitor 1–3%, mutual solvent 0.1–20% and the rest is water. The acid is to cause corrosion and pores in the formation, the cobalt and/or nickel salt act as catalysts to promote the pyrolysis of kerogen, the inhibitor is to keep the treatment steady and prevent corrosion of metal pipes.

The preparation of the treatment agent included the following steps:

1) calculating the amount of each component required according to the treatment agent formula designed, and weighing the components;
2) adding respectively the acid, cobalt salt, nickel salt, inhibitor and mutual solvent to the 2/3–4/5 portion of the required amount of water with stirring while adding;
3) adding the remaining water to the above mixtures and preparing the treatment agents by thoroughly stirring and mixing.

In this study, three different treatment agents were designed and prepared, and were named treatment agents A, B and C, respectively.

The performance test of treatment agents included the following stages:

1) crushing and screening Maoming oil shale samples and selecting samples of a particle size of 3.35–4.75 mm, weighing 30 g of the samples and placing them in a plastic bottle;
2) pouring 100 mL of the prepared treatment agent into the bottle and placing it in the environment of 40 °C for 2 h to let the agent react with oil shale particles, discarding the treatment agent after the reaction was complete;
3) washing the samples with water and placing them thereafter in the drying oven at 105 °C for 4 h;
4) weighing 5 g of samples dried in stage 3, observing the samples with an optical microscope after natural cooling to room temperature, testing the pore size distribution and porosity of the samples by a 3H-2000PS1 specific surface area and pore size distribution analyzer;
5) weighing 15 g of samples dried in stage 3 and placing them in the vacuum reactor at 350 °C for 65 h to pyrolyze the organic of oil shale samples during the heating process, collecting and measuring pyrolysis oil and gas and calculating the oil recovery;
6) observing the samples with an optical microscope after pyrolysis and natural cooling, testing the pore size distribution and porosity with a 3H-2000PS1 specific surface area and pore size distribution analyzer.

In this study, the oil shale samples treated with treatment agents A, B or C are named samples A, B or C, respectively. A contrast experiment was performed and would only run through test stages 1, 3, 4, 5 and 6. In the contrast experiment, the oil shale sample used was the original sample.

3. Results and discussion

3.1. Pulse power fracturing technology

According to the results of the study of rock mechanical properties, its breaking limit at high-acceleration shock load is significantly lower than that under static load. The peak pressure of the shock wave generated by the electric pulse device is higher than 100 MPa (Fig. 1), impacting the reservoir at a several-thousand-fold acceleration of gravity. Under this high-acceleration shock wave, the impact strength is much higher than the fatigue strength of rock, which can extend the existing fractures and generate micro- or macrofractures until the impact strength is reduced to the fatigue strength of rock. These new fractures will increase the permeability of the reservoir.

PPFT was successfully applied to the sandstone sample and farmland. Figure 2 illustrates the results of the laboratory test conducted on the sandstone sample by using the electric pulse device. It can be seen from the figure that the sandstone sample was well fractured under the impact of shock waves generated by the electric pulse device for five times. Each time one bullet with the energy of 30 kJ was used. Figure 3 shows the results of the field test on the farmland where the energy of each bullet was increased to 90 kJ. As shown in Figure 3, the farmland can be fractured by only one shot. The depth applied in this test was about 2 m.

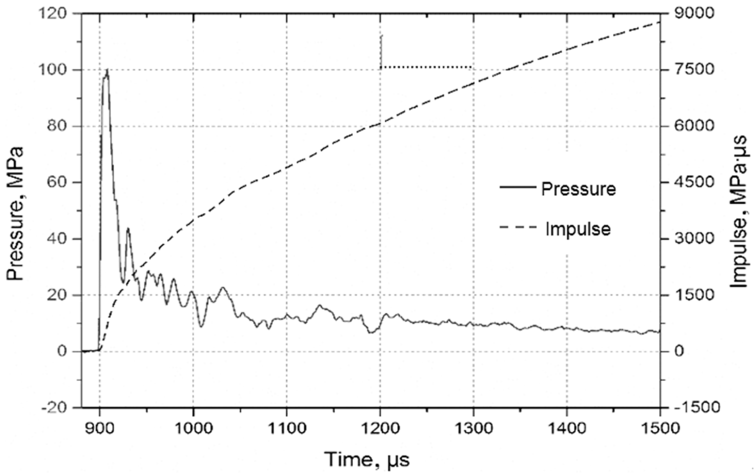

Fig. 1. Energy release process of the repeat pulse shock wave.

Fig. 2. Laboratory test on the sandstone sample (30 kJ for five times).

Fig. 3. Field test on the farmland (90 kJ once).

For Maoming oil shale, its richness in clay minerals, shallow depth of the main seam and well-developed horizontal beddings enable only horizontal fractures to be easily formed, while the effect of stimulation using hydraulic fracturing is low. In contrast, the effect of using PPFT is higher.

Well MYY-1 is an oil shale coring and test well of SINOPEC in the Maoming block. In September 2015, PPFT was applied to the well, and its effect was tested. Figure 4 shows the logging curves of well MYY-1.

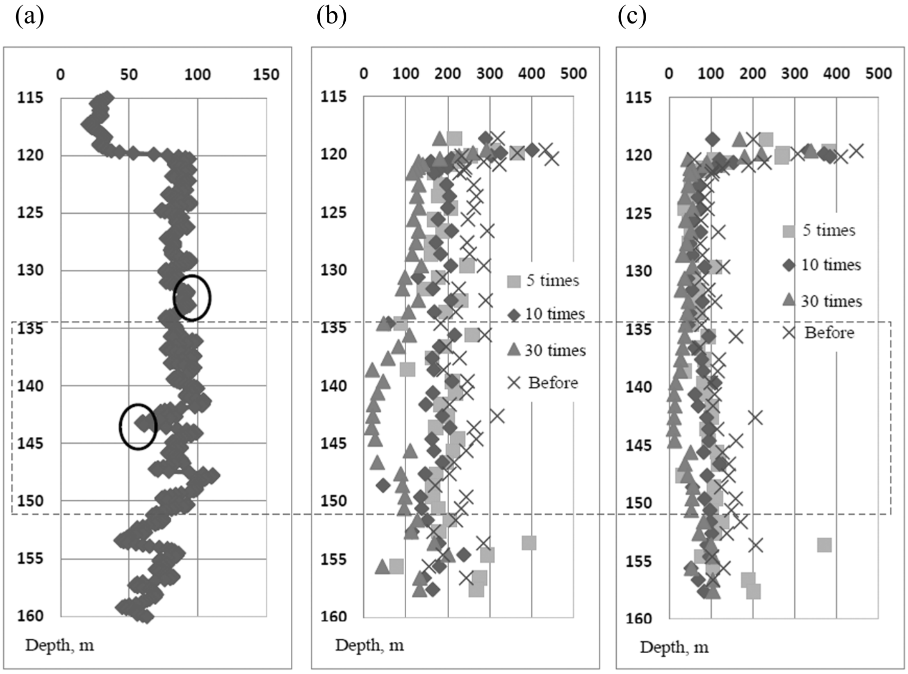

Fig. 4. The logging curves for well MYY-1: (a) natural gamma logging curve; (b) upper ultrasonic test curve; (c) under ultrasonic test curve.

Figure 4a displays the natural gamma logging curve of well MYY-1 without applying PPFT. The top depth of the oil shale formation is 120 m, and the bottom depth, 160 m. Two acting positions of the shock wave were designed. The first one, with a relatively low natural gamma value, was at a depth of 143 m. The second one, with a relatively high natural gamma value, was at a depth of 132 m. For the first acting position, the shock wave was applied 40 times, each time using a bullet with the energy of 120 kJ. For the second acting position, the shock wave was applied 48 times and 48 bullets were used (22 bullets of 120 kJ, 26 bullets of 30 kJ). Figures 4b–c show respectively upper and under ultrasonic test curves of well MYY-1 before and after applying PPFT in the first acting position. The ultrasonic test used a single transmitter with a double receiver, observing two ultrasonic test curves. It can be seen from Figure 4 that the ultrasonic test curves are consistent with the natural gamma logging curve. The upper and under ultrasonic test values decreased with time, especially when the shock wave was applied 30 times, the ultrasonic test values decreased rapidly. A low ultrasonic test value suggests the development of fractures. The tests demonstrated that PPFT can break the oil shale formation effectively and the retrofit distance may exceed 15 m. For the second acting position, the pattern of change of ultrasonic test values was similar.

The hydraulic pressure drop test was also carried out to uncover the effect of PPFT. The results are shown in Figure 5. Before stimulation, the pumping pressure drops slowly, which indicates that the permeability of the formation is very low. After stimulation in the first acting position, the fall-off speed of the pumping pressure increases obviously. After stimulation in the first and second positions, the pumping pressure drops more quickly. These results demonstrate that PPFT significantly contributes to increasing the permeability of the oil shale formation.

Theoretical research and laboratory test results indicate that PPFT can be applied to different formations, such as sandstone, oil shale, etc.

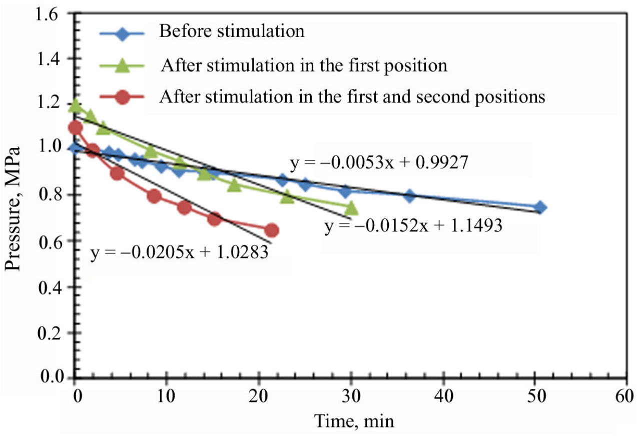

Fig. 5. The hydraulic pressure drop test curves for well MYY-1.

3.2. Treatment agent post-processing technology

The experimental results obtained employing the treatment agent post-processing technology (TAPT) are illustratively shown in Figures 6, 7 and 8 and presented in Table 3. Figure 6 shows images of original (untreated) and treated oil shale samples as observed by an optical microscope. As can be seen from the figure, the original sample is very compact (Fig. 6a), while samples A, B and C treated by treatment agents A, B and C, respectively, have become loose with developed microfractures (Figs. 6b–d).

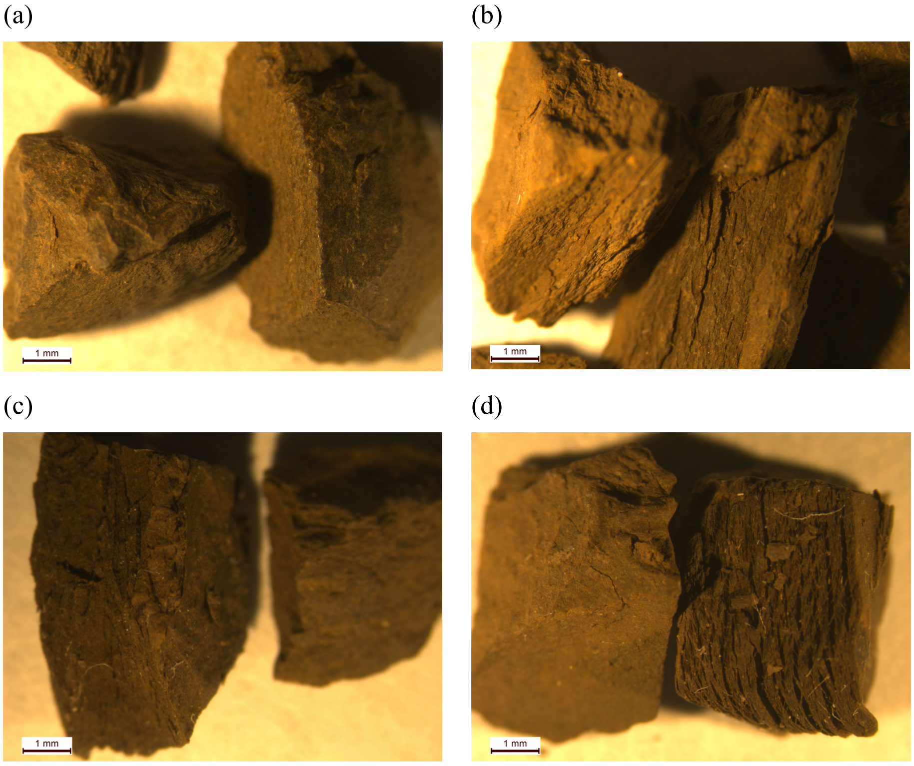

Fig. 6. Optical microscopic images of oil shale samples before and after treatment: (a) original sample; (b) sample A; (c) sample B; (d) sample C.

The effect of different treatments on pyrolyzed oil shale samples is illustrated in Figure 7. It can be seen that the original sample, after heating and pyrolysis, is still compact with only few fractures developed (Fig. 7a), but in samples A, B and C, a complex network of fractures has formed after pyrolysis (Figs. 7b–d).

Figure 8 shows the pore size distribution of different oil shale samples before and after pyrolysis by using a 3H-2000PS1 specific surface area and pore size distribution analyzer. The instrument employs the static volumetric

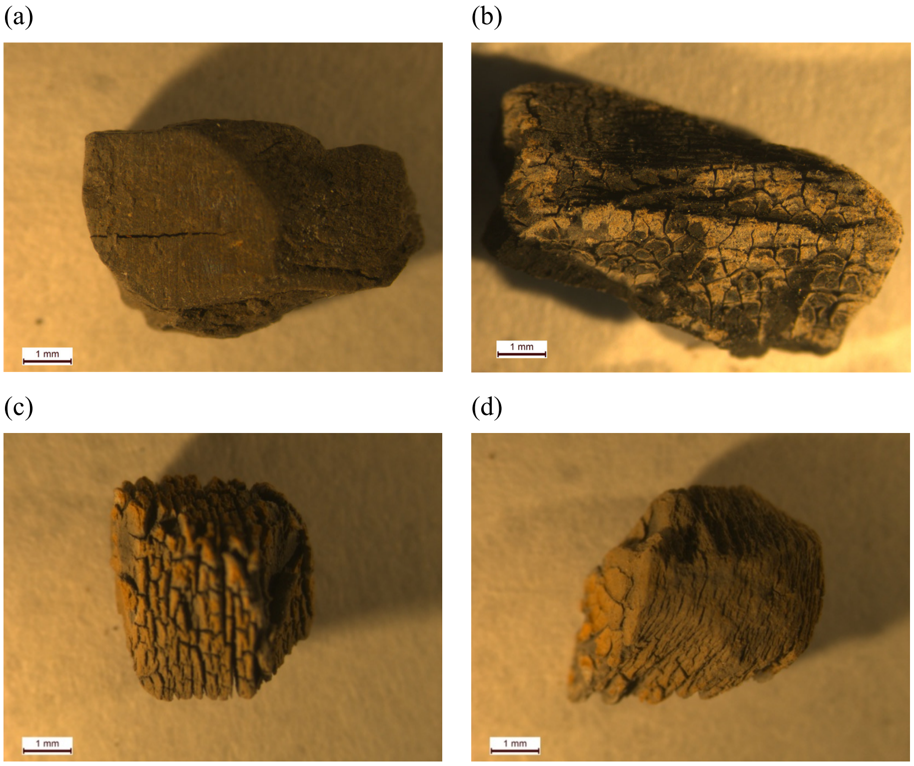

Fig. 7. Effect of treatment on pyrolyzed oil shale samples: (a) pyrolytic original sample; (b) pyrolytic sample A; (c) pyrolytic sample B; (d) pyrolytic sample C.

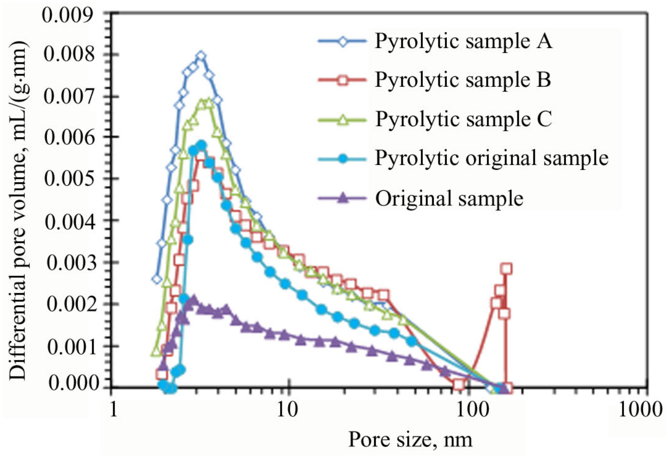

Fig. 8. The pore size distribution of different oil shale samples before and after pyrolysis.

Table 3. Effect of treatment on oil shale porosity and oil recovery

	Porosity before pyrolysis, %	Porosity after pyrolysis, %	Oil recovery*, %
Original sample	14.3	19.9	29
Sample A	15.1	22.7	37
Sample B	15.6	27.3	40
Sample C	15.4	24.9	39

* compared with oil yield in Fischer assay.

method (nitrogen adsorption and desorption) and its pore size test range of 0.35–200 nm enables detecting micro-, meso- and macropores. From Figure 8 it can be seen that compared to the samples before pyrolysis, the amount of micro-, meso- and macropores in all of them after pyrolysis has increased, while this trend is more evident in the samples treated by treatment agents A, B and C, respectively.

The 3H-2000PS1 specific surface area and pore size distribution analyzer can also be used to investigate porosity (0.35–200 nm pores). The pertinent results for oil shale samples before and after pyrolysis and oil recovery are presented in Table 3. The porosity and oil recovery were increased if the oil shale sample had been treated by the treatment agent, whereas the effect of treatment agent B was the most obvious.

The above results show that for Maoming oil shale, the treatment agents developed in this study can remarkably promote the formation of fractures, increase porosity and permeability and enhance pyrolysis.

4. Conclusions

1) Pulse power fracturing technology (PPFT) was designed and applied to well MYY-1 in the Maoming block, South China. Both the ultrasonic wave test and the hydraulic pressure drop test were conducted to assess the effect of stimulation on the oil shale formation. The results demonstrated that by employing PPFT one can effectively break the oil shale formation, while the effect distance may exceed 15 m.
2) Three different treatment agents were designed and their performance was experimentally assessed. The results demonstrated that for Maoming oil shale, these treatment agents remarkably promoted the development of fractures and increased its porosity and permeability, thereby boosting pyrolysis. Based on these findings, the treatment agent post-processing technology (TAPT) was developed.
3) Both PPFT and TAPT contribute to increasing the permeability of oil shale formations. Hence, these technologies may have great potential for the in-situ exploitation of oil shale resources employing thermal fluid heating.

Acknowledgements

This study was supported by the program "Research on variation properties of oil shale during in-situ heating with thermal fluids" (G5800-15-ZS-KJB026) of the Petroleum Exploration and Production Research Institute of SINOPEC, China.

REFERENCES

1. Bunger, J. W., Crawford, P. M., Johnson, H. R. Is oil shale America's answer to peak-oil challenge? *Oil Gas J.*, 2004, **102**(8), 16–24.
2. Dyni, J. R. *Geology and Resources of Some World Oil-Shale Deposits*. Scientific Investigations Report 2005-5294. US Geological Survey, Reston, Virginia, 2006.
3. Liu, Z. J., Dong, Q. S., Ye, S. Q., Zhu, J. W., Guo, W., Li, D. C., Liu, R., Zhang, H. L., Du, J. F. The situation of oil shale resources in China. *Journal of Jilin University (Earth Science Edition)*, 2006, **36**(6), 869–876 (in Chinese with English abstract).
4. Guo, Y. G., Xu, X. Q., Wang, H. Y., Zheng, D. W., Zhang, Y. G., Hou, Q. H. Research progress in use of oil shale as an unconventional energy. *Jiangsu Chemical Industry*, 2008, **36**(2), 6–9 (in Chinese).
5. Fang, C. H., Zheng, D. W., Liu, D. X., Wang, Y. F., Xue, H. Q. The development and trends about in-situ mining technology of oil shale. *Energy Technology and Management*, 2009, (2), 78–80 (in Chinese).
6. Feng, X. W., Chen, C., Chen, D. Y. New development of oil shale in-situ technology. *China Mining Magazine*, 2011, **20**(6), 84–87 (in Chinese).
7. Vinegar, H. Shell's *in-situ* conversion process for oil shale. *26th Oil Shale Symposium*, Colorado School of Mines, 16–20 October 2006, Colorado, USA.
8. Yang, H., Gao, X. Q., Xiong, F. S., Zhang, J. L., Li, Y. J. Temperature distribution simulation and optimization design of electric heater for in-situ oil shale heating. *Oil Shale*, 2014, **31**(2), 105–120.
9. Tanaka, P. L., Yeakel, J. D., Symington, W. A., Spiecker, P. M., Del Pico, M., Thomas, M. M., Sullivan, K. B., Stone, M. T. Plan to test ExxonMobil's in situ oil shale technology on a proposed RD&D lease. *31st Oil Shale Symposium*, Colorado School of Mines, 17–19 October 2011, Colorado, USA.
10. Looney, M. D., Polzer, R., Yoshioka, K., Minnery, G. Chevron's plans for rubblization of Green River Formation oil shale (GROS) for chemical conversion. *31st Oil Shale Symposium*, Colorado School of Mines, 17–19 October 2011, Colorado, USA.
11. Allix, P., Burnham, A. K., Fowler, T., Herron, M., Kleinberg, R., Symington, B. Coaxing oil from shale. *Oilfield Review (Schlumberger)*, Winter 2010/2011, **22**(4), 4–15.
12. Qian, J. L., Yin, L., Wang, J. Q., Li, S. Y., Han, F., He, Y. G. *Oil Shale: Supplementary Energy of Petroleum*. Sinopec Press, Beijing, 2008, 71 (in Chinese).
13. Yutkin, L. A. *Electrohydraulic Effect* (Yu, J. S., transl.) Science Publishing House, Beijing, 1962 (in Chinese).
14. Bai, X. Y., Sun, G. Z. Application of impulse discharging on cleanout of wells. *Oil-Gas Field Surface Engineering*, 1996, **15**(3), 8–10 (in Chinese).

Presented by S. Li
Received December 21, 2015